Checking graphite and stainless anodes with an experimental model of marine microbial fuel cell

Claire Dumas[a], Alfonso Mollica[b], Damien Féron[c], Régine Basseguy[a], Luc Etcheverry[a] and Alain Bergel[a]

[a]Laboratoire de Génie Chimique CNRS-INPT, 5 rue Paulin Talabot, BP 1301, 31106 Toulouse, France
[b]CNR-ISMAR, via de Marini 6, 16149 Genoa, Italy
[c]SCCME, CEA Saclay, Bat 458, 91191 Gif-sur-Yvette, France

Abstract

A procedure was proposed to mimic marine microbial fuel cell (MFC) in liquid phase. A graphite anode and a stainless steel cathode which have been proven, separately, to be efficient in MFC were investigated. A closed anodic compartment was inoculated with sediments, filled with deoxygenated seawater and fed with milk to recover the sediment's sulphide concentration. A stainless steel cathode, immersed in aerated seawater, used the marine biofilm formed on its surface to catalyze oxygen reduction. The cell implemented with a 0.02 m^2-graphite anode supplied around 0.10 W/m^2 for 45 days. A power of 0.02 W/m^2 was obtained after the anode replacement by a 0.06 m^2-stainless steel electrode. The cell lost its capacity to make a motor turn after one day of operation, but recovered its full efficiency after a few days in open circuit. The evolution of the kinetic properties of stainless steel was identified as responsible for the power limitation.

Keywords : Microbial fuel cell; Stainless steel; Sediments; Impedance spectroscopy

1. Introduction

Microorganisms contained in different natural environments are able to form biofilms on electrode surfaces and oxidize organic matter using the electrode as direct electron acceptor, without the presence of any artificial mediator. Microbial fuel cells (MFCs) take advantage of this property to harvest electricity from a wide range of organic waste or renewable biomass. They offer promising advantages with respect to standard abiotic fuel cells: naturally grown microorganisms replace the expensive catalysts required in traditional fuel cells; bacteria adapt to different organic matters and can work in "dirty" natural and industrial environments such as wastewater or sediments ([Lovley, 2006a] and [Lovley, 2006b]). The literature on this topic has been exhaustively reviewed from the point of view of either microbial mechanisms and ecology ([Angenent et al., 2004], [Logan and Regan, 2006] and [Rabaey and Verstraete, 2005]), or engineering and technological aspects ([Logan et al., 2006], [Lovley, 2006a] and [Lovley, 2006b]).

Environmental MFCs were first implemented in marine sediments with graphite anodes. The power supplied were around 0.02 W/m^2 in field conditions (Tender et al., 2002) whereas laboratory sediment fuel cells reached 0.01 W/m^2 (Reimers et al., 2001). Power has been increased up to 0.10 W/m^2 by improving the anode material, using (anthraquinone-1,6-disulfonic acid)-modified graphite or graphite powder compressed with manganese and nickel salts (Lowy et al., 2006) as mediators. In wastewater treatment plants, MFCs have demonstrated the ability to produce simultaneously energy (0.49 W/m^2) and enhance the degradation of organic matter (Liu and Logan, 2004). Higher power values have been reached with optimal procedures. Power densities up to 4.31 W/m^2 were obtained with high biomass concentration of mixed cultures from potato processing sludge fed with glucose ([Rabaey et al., 2003] and [Rabaey et al., 2004]). Most of the environmental MFC studies have focused the anodic part and avoided limitation from the cathode, by using platinum-based catalysts for oxygen reduction, or adding hexacyanoferrate as final electron acceptor. These systems are efficient for laboratory cells but would not be sustainable for large-scale pilots. A few studies dealt with microbial-catalyzed cathode processes ([Park et al., 2005] and [Rhoads et al., 2005]). In a previous work (Bergel et al., 2005), we demonstrated that a biofilm formed in seawater on a stainless steel cathode catalyzes oxygen reduction in a hydrogen PEM fuel cell. The biofilm-covered stainless steel cathode was able to sustain 0.06 W/m^2 with a current density of 1890 mA/m^2.
The purpose of this work was to design a MFC prototype with such a biofilm stainless steel cathode, and graphite or stainless steel as anode. Using stainless steel for both electrodes would be an important advantage with the view to scale-up industrial MFC, because of the commercial availability of this material, which would allow designing volumetric electrodes with high mechanical properties and good long-term behaviour. The cathode must be implemented in aerated seawater and the anode in sediment, as commonly done for benthic MFCs. Nevertheless, the practical problems linked to experimenting directly in the field with the anode embedded in deep submarine sediments (Dumas et al., 2007) were avoided here by using a laboratory model that mimicked sediments/seawater environments. This experimental model has already been used with success in the domain of microbial corrosion, and it may propose a suitable solution to develop marine MFCs before testing them in seas and oceans.

2. Methods

2.1. Microbial fuel cell

The marine microbial fuel cell prototype was set-up in a station in Genoa harbour close to the sea. The 20 × 30 cm stainless steel cathode (UNS S31254; Cr, 19.9%; Ni, 17.8%; Mo, 6.0%; N, 0.2%; C, 0.01%; Fe, complement) was plunged into a 100 l aquarium of seawater continuously renewed (6 l/h) and thermostatically maintained at 25 °C. A zinc electrode placed in the cathodic compartment was coupled with the stainless steel cathode to help the cathodic biofilm development during the preparation phase. During experiments, it was used in some cases as a pseudo-reference electrode. Anodes were either 20 mm-thick sheets of graphite (200 cm^2 – Goodfellow) or 3 mm-thick sheets of stainless steel (UNS S31254, 600 cm^2 – Outokumpu). The anode was dipped in a closed 35 l tank that contained around 0.2 l marine sediments collected at 15 m under the water surface completed with seawater. A cotton mesh ensured ionic connection between the anode and cathode compartments. At the beginning of experiments, oxygen was

eliminated from the anode tank by the addition of sulphite (Na_2SO_3) in excess. During the sediments preparation, milk was added every 2 or 3 days and was stopped when sulphite concentration reached a value close to the concentration in natural marine sediments (300–400 ppm). Milk was also added during the experiments with the graphite anode. Cathode and anode were connected through an electrical motor or with electrical resistances varying from 1 Ω to 33 kΩ.

2.2. Electrochemical monitoring

The voltage drop between anode and cathode (ΔV) and the cathode potential (E_C) with respect to a silver/silver chloride (Ag/AgCl) reference electrode were measured every hour. At open circuit, both anode and cathode potentials were measured with respect to the reference electrode. The data acquisition system consisted of a PCI-6034E (National Instrument) acquisition card monitored via a Labview6 graphic interface. When indicated, an electrical motor was used, which turned a propeller. The motor internal resistance was 25 Ω, and the propeller turned when the system provided at least 0.15 V, i.e. to turn the propeller, the system must sustain at least 6 mA.

2.3. Analytical methods

Energy dispersive spectroscopy (EDS) was performed on stainless steel samples with a SiLi energy dispersive probe (Link Analytical mod E5526) from the EDAX Company.
Mott–Schottky tests were performed with a frequency response analyzer (Schlumberger 1255) coupled with a potentiostat (Schlumberger 1286). Measurements were carried out at 1592 Hz with amplitude of 10 mV and integration time of 0.1 s; potential was scanned starting from −0.50 V to 0.00 V vs. Ag/AgCl by steps of 50 mV. Stainless steel electrodes are covered by a passive layer composed of metallic oxides that has semi conductive features. The charge distribution at the stainless steel/electrolyte interface was determined by measuring the capacitance of the passive layer C_{pl} as a function of electrode potential E according to the Mott–Schottky relationship (L'Hostis et al., 2003).

3. Results and discussion

3.1. Graphite anode

The 35 l anode tank was inoculated with 0.2 l marine sediments collected at 15 m under the water surface, and filled with seawater. Oxygen was fast eliminated by the addition of sulphite (Na_2SO_3) in excess. The oxidation of sulphide to sulphur

(1)
$HS^- \rightarrow S^0 + H^+ + 2e^-$
has a crucial importance in controlling the electrochemical phenomena that can occur in sediments. In the framework of microbial corrosion, the concentration of sulphide is one of the key parameter to be monitored. Sulphide has also been believed to play a key role in benthic MFCs, as they produce an important part of the current due to electrochemical oxidation on the

anode ([Lovley, 2006a], [Lovley, 2006b], [Orfei et al., 2006] and [Ryckelinck et al., 2005]). For this reason, the sulphide concentration was focused here to obtain an environment in the anode compartment as close as possible to the conditions in sediments. Sulphate reducing bacteria are known to convert the sulphate ions contained in seawater to sulphide (HS^-; Jorgensen, 1977) and they use efficiently milk as nutrient. Consequently, milk was added in the anode tank to promote the activity of sulphate reducing bacteria in converting sulphate to sulphite. Milk was added approximately every 2 days, and feeding was stopped when sulphite concentration reached a value similar to the concentration in natural marine sediments, in the range 300–400 ppm, when the concentration of sulphide in the tank was close to the natural concentration in sediments and the pH close to 6.5–6.7, the medium was considered to be ready for implementing in the microbial fuel cell (MFC). This experimental model had revealed to be efficient to reproduce in the laboratory the microbial corrosion of steels that occurs in natural marine sediments (Mollica, 2000).

The closed anode tank was immersed in an open basin where seawater was continuously renewed (cathode basin). Anode and cathode were individually prepared. The 10 × 20 cm graphite anode was kept at open circuit for 4 days in the anode tank. Its potential remained stable around −0.40 V vs. Ag/AgCl. At the same time, a 20 × 30 cm stainless steel cathode was set-up in the seawater cathode basin and coupled through a 50 Ω resistance to a zinc electrode also immerged in the seawater basin. The zinc electrode spontaneously dissolves in seawater:

(2)
$$Zn^{2+} + 2e^- \rightarrow Zn \quad E^0_{Zn} = -0.98 \text{ V vs. Ag/AgCl}$$

and ensures a negative potential value on the cathode that maintained active O_2 reduction. These conditions promote the formation of electrochemically active biofilm on the cathode that have been revealed to be remarkably efficient for oxygen reduction (Bergel et al., 2005). The cathode potential increased from around −0.60 V to 0.00 V vs. Ag/AgCl in 3.5 days. Resistance was then lowered to 25 Ω and potential went to −0.10 V vs. Ag/AgCl. The cathodic current increased from around 3 mA to 19 mA (300 mA/m^2 with respect to the projected surface area of the cathode), which confirmed the usual formation of an aerobic electrochemically active biofilm (Bergel et al., 2005).

After the preparation phase, the microbial fuel cell was started by disconnecting the stainless steel cathode from the zinc electrode, and connecting the graphite anode and the stainless steel cathode through the electric motor that runs a propeller. Power remained stable around 3 mW for the first 25 days, which represented 0.15 W/m^2 with respect to the anode projected surface area (Fig. 1A). At least 0.10 W/m^2 was sustained for 45 days. Moreover, the propeller turned along the two month length of the experiment, except for days 1, 17 and 18. Anode and cathode potentials were monitored each vs. an Ag/AgCl reference electrode, set in the anode tank and in the cathode basin, respectively. Potential monitoring (Fig. 1B) showed that decreases in power were due to a drastic deficiency of the cathode, whose potential decreased from around 0.20 V vs. Ag/AgCl to −0.40 V vs. Ag/AgCl. Nevertheless, the cathode rapidly recovered on its own. Microscopic observations indicated that these transient decreases were probably due to an anomalous development in the seawater basin of grazing organisms (briozoa) that consumed the biofilm on the stainless steel surface. To our knowledge this problem has never been evoked before, but it may take a high importance with the view to develop such stainless steel cathodes in large-scale marine MFCs.

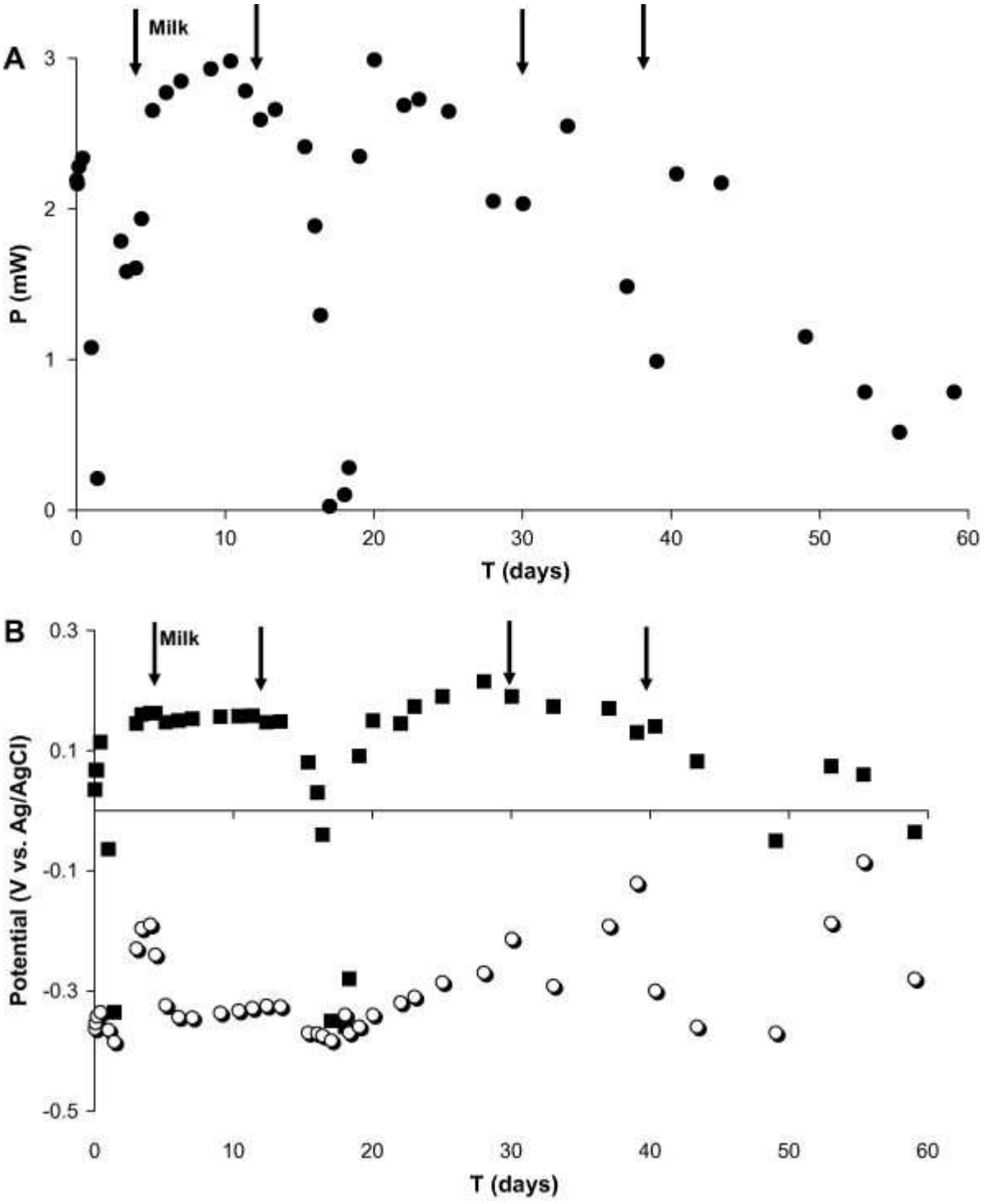

Fig. 1. MFC with graphite anode and stainless steel cathode. Arrows indicate addition of milk in the anodic tank. (A) Power (mW) supplied vs. time (days) during motor running. (B) Potential (V vs. Ag/AgCl) of the graphite anode (0.02 m^2; (○)) and stainless steel cathode (0.06 m^2; (■)) when connected through the propeller (25 Ω).

Fig. 1B also shows that small decreases in anode efficiency were corrected by the addition of around 10 ml milk on days 4, 12, 30 and 39. Anode limitations were due in this case to substrate depletion in the tank. This addition of substrate maintained the efficiency of the anode.
On day 42, when power was around 2.2 mW, the electrodes were transiently disconnected and connected to a potentiostat with an auxiliary electrode and an Ag/AgCl reference to record current–potential curves of both anode and cathode. The open circuit potential of the graphite anode was −0.33 V vs. Ag/AgCl and the maximum current 70 mA obtained at 0.00 V vs. Ag/AgCl corresponded to 3500 mA/m^2 (Fig. 2). The current–potential curves confirmed that the cell was limited by the lower efficiency of the stainless steel cathode. Its open circuit potential was lower than previously obtained in similar conditions, around up to +0.20 V vs. SCE, i.e. 0.21 V vs. Ag/AgCl, and it did not sustain the current density previously reached up to 500 mA/m^2 (Bergel et al., 2005). On the contrary, the anode model, which allowed sustaining 0.15 W/m^2 for around one month, certainly overestimated the power that can be supplied by natural sediment, because of milk addition. Working in liquid medium rather than in solid sediments may also be another cause of the high power density, because of enhanced mass transfer. Generally, values obtained in literature with sediments have been reported close to 0.01 W/m^2 (Reimers et al., 2001), 0.02 W/m^2 (Tender et al., 2002) or up to 0.10 W/m^2 with graphite anode modified with electrochemical mediators (Lowy et al., 2006). Nevertheless, the milk addition was required in order to get the sulphide concentrations in the experimental model of the same order of magnitude than in sediments. Thanks to this condition, the model revealed to be efficient in maintaining the potential of the anode close to values recorded in natural sediments, around −0.4 V vs. Ag/AgCl ([Orfei et al., 2006], [Reimers et al., 2006] and [Ryckelinck et al., 2005]). It will so be further used to test stainless steel anodes.

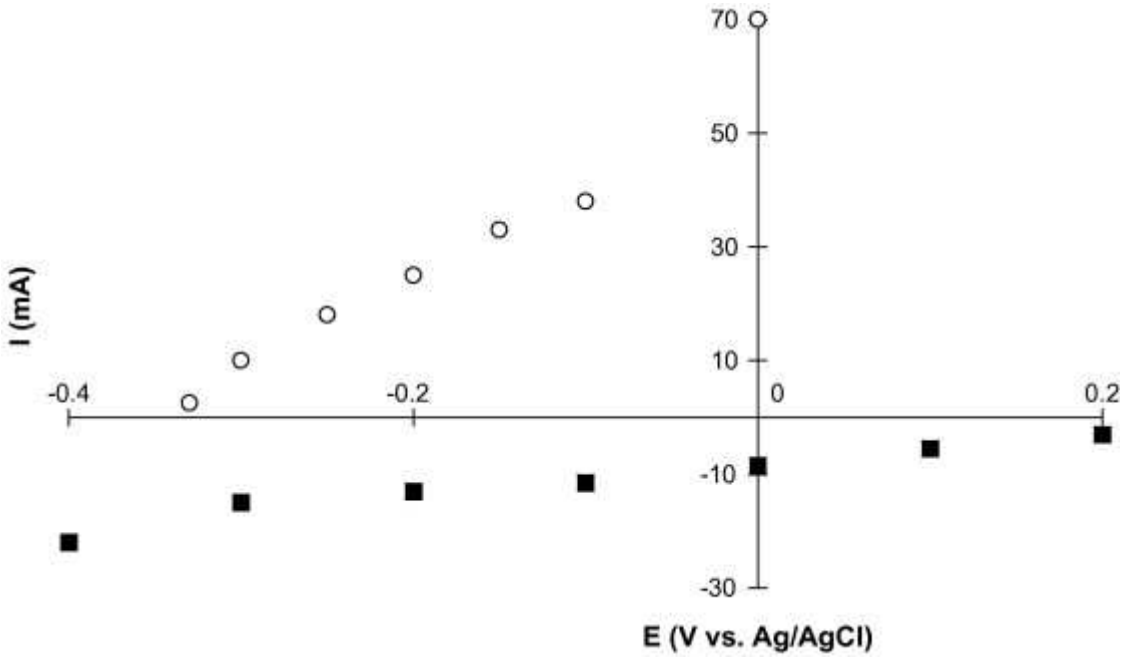

Fig. 2. Polarization curves obtained with a graphite anode (0.02 m^2; (○)) and a stainless steel cathode (0.06 m^2; (■)). The anode and cathode surface areas were different the current was consequently reported in mA instead of current density.

3.2. Power generation with a stainless steel anode

The anode tank was refilled with fresh seawater and sediment inoculum and prepared following the procedure described above. A 20 × 30 cm stainless steel anode was placed in the closed anode tank and left in open circuit. The stainless steel cathode was coupled to a zinc electrode until day 13 to form the cathodic biofilm. At day 13, the cathode was disconnected from the zinc electrode and coupled to the anode through the electrical motor. The propeller started to turn but stopped after one complete day of operation. After six days back in open circuit, polarization curves were plotted on day 20 by connecting the electrodes through electric resistances of different values (Fig. 3). The motor was connected again to the cell and turned for more than an hour. It remained connected all day and new polarization curves were plotted on day 21. Electrodes were then left on open circuit for four days, and the last polarization curves were plotted on day 25. Current density values were calculated with respect to the projected electrode surface area of 0.06 m^2 for both anode and cathode. All cathodic curves were nearly identical, meaning that cathode behaviour was not influenced by the motor operation. The open circuit potential values in the range 0.30–0.35 V vs. Ag/AgCl demonstrated an effective catalysis of oxygen reduction by the biofilm. The current values obtained, around 100 mA/m^2 at 0.00 V vs. Ag/AgCl, were of the same order of magnitude as that obtained elsewhere in similar quiescent conditions (250 mA/m^2 at −0.10 V vs. SCE (Bergel et al., 2005)).

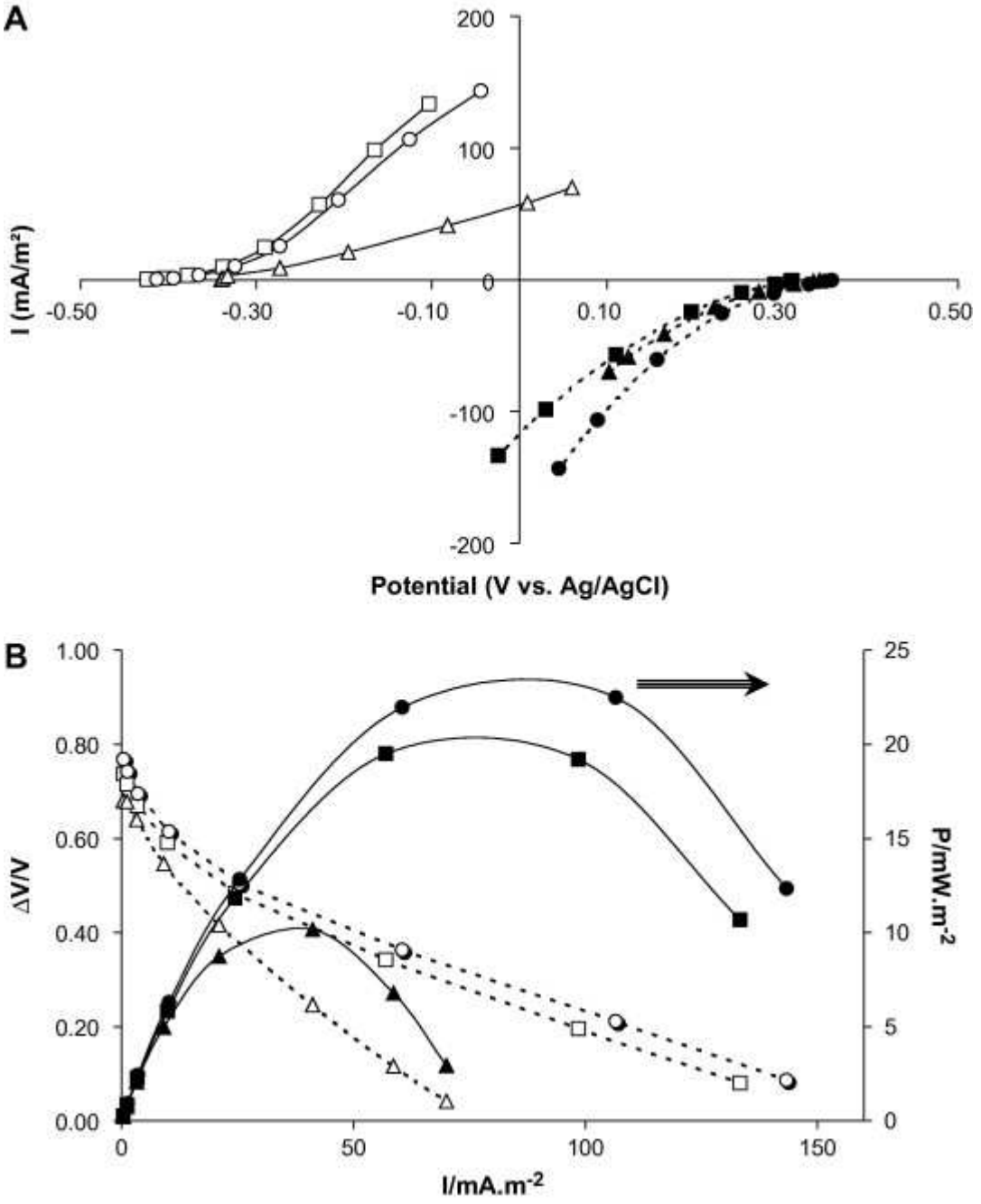

Fig. 3. Characterization of the MFC with stainless steel anode and cathode at day 20 (□) after open circuit; day 21 (Δ) after one day connection to the motor; day 25 (○) after four days in open circuit. (A) Current density (mA/m^2) vs. potential (V vs. Ag/AgCl). Black and white symbols represent cathode and anode curves, respectively. (B) Power density (mW/m^2) and potential drop (ΔV) vs. current density (mA/m^2). Black and white symbols represent power and potential drop values, respectively.

In contrast, the anode features were markedly affected by the motor operation. After one day of motor connection the polarization curve slope decreased (day 21). The anode could no longer sustain more than 70 mA/m^2, which was not sufficient for the propeller to turn. Actually, to be in action, the propeller required a current of 6 mA, i.e. a current density of 100 mA/m^2 in this context. The polarization curve plotted at day 25 showed that the anode had recovered its full capacity to provide current after four days in open circuit (motor disconnected). Loss/recovery of its power capacity was fully reversible. The maximum power density supplied by the MFC at day 25 was around 0.02 W/m^2 with approximatively 85 mA/m^2 (Fig. 3B). The reversible limitation in power supplied cannot be attributed to the transient depletion of the substrate in the vicinity of the anode surface, as in similar conditions the graphite anode supplied continuously at least 0.1 W/m^2 for 45 days.

3.3. Further investigations with stainless steel anodes

At day 35, two small clean stainless steel electrodes, 2.5 cm^2 surface area each, were added into the anode tank. One was left in open circuit while the second was continuously polarized at −0.10 V vs. Ag/AgCl, value of the anode potential where high current densities were obtained (Fig. 3). The current was periodically recorded, and reported in Fig. 4A on a log(*i*) vs. log(*t*) scale. The initial biofilm-covered anode (0.06 m^2), which had been in the same tank since the beginning of the tests and was repeatedly used to generate motor rotation, was also periodically polarized at −0.10 V vs. Ag/AgCl as follows:

– after 3, 7, 10.5, 25 and 48 h from the beginning of this experiment, the electrode was polarized for only 10 min, and the current was recorded at the end of each short polarization,

– after 48 h, polarization was applied continuously.

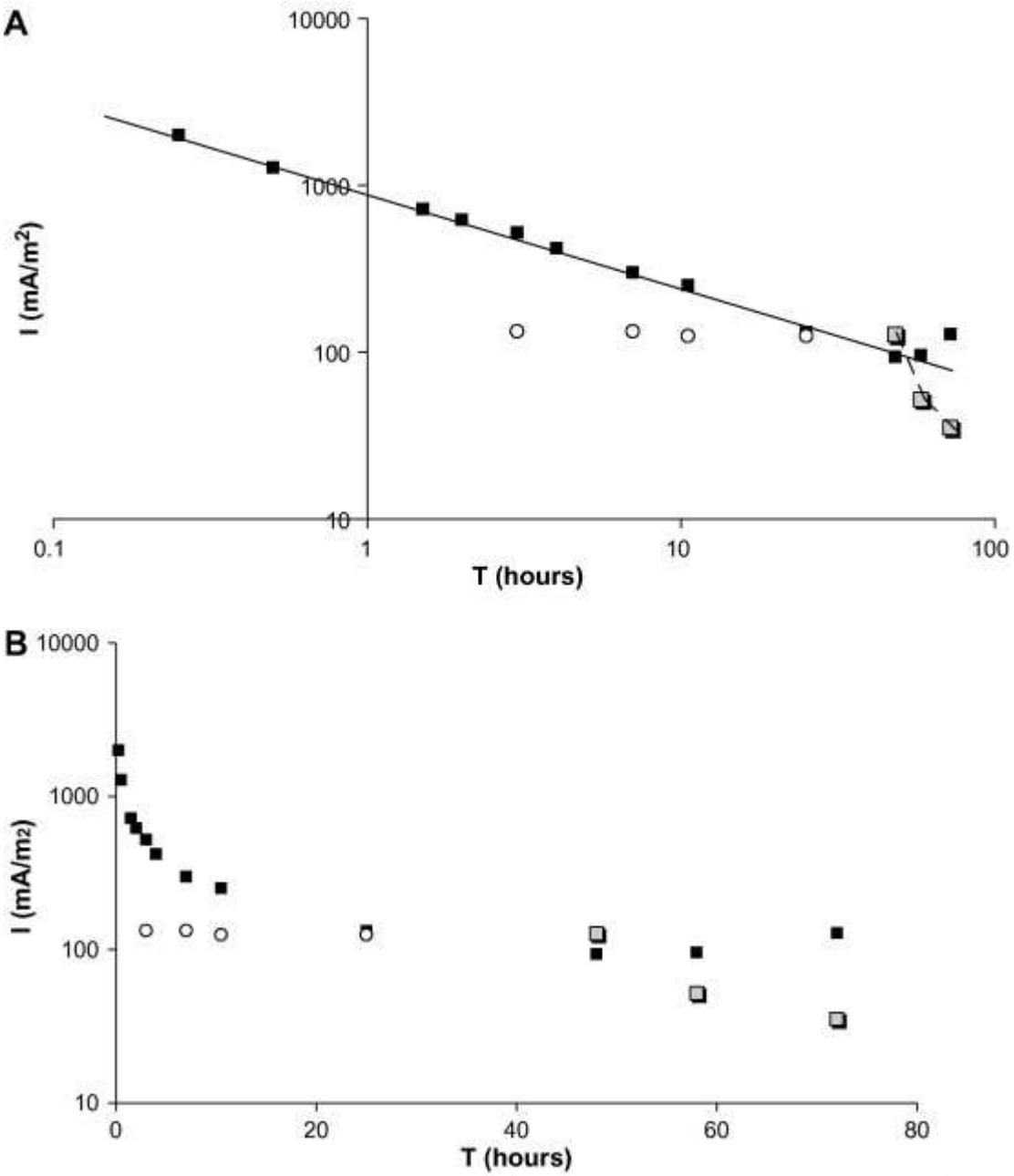

Fig. 4. Evolution of current density (mA/m^2) with a new clean electrode (2.5 cm^2) polarized at −100 mV vs. Ag/AgCl (■); biofilm-covered electrode polarized intermittently (○) and continuously after 48 h (■); interpolation of results: (▬) $i = 840 \times t^{-0.5}$; (▬ ▬) $i = 180 \times (t - 46)^{-0.5}$. (A) In a log–log scale. (B) In a log–regular scale.

The small clean electrode placed under constant polarization gave a linear current decrease in log–log scale from around 1500 mA/m^2 to 100 mA/m^2, that fitted a relationship in $t^{-0.5}$ (the line in Fig. 4A corresponds to $i = 840 \times t^{-0.5}$; i expressed in mA/m^2, t in hours). On the contrary, the initial electrode, with only 10 min of periodical polarization, gave a constant current density around 125 mA/m^2. After 48 h, the initial electrode was polarized continuously and exhibited a continuous current decrease, in agreement with the $t^{-0.5}$ relationship (the line in Fig. 4A

corresponds to $i = 180 \times (t - 46)^{-0.5}$; i expressed in mA/m^2, t in hours). The constant value of current density that was recorded during successive intermittent polarizations with the initial biofilm-covered electrode confirmed that there was no significant modification in the medium composition, and particularly no substrate depletion. Moreover, when the small electrode that was continuously polarized was briefly moved in order to renew the medium around it, no variation in current was registered. Substrate depletion should be described by an exponential law such as $i = A \times \exp(-B \times t)$ that would give linear evolution in a log(i) vs. t representation, but this was not the case, as shown in Fig. 4B. As a consequence, the current density decrease that was observed only under constant polarization was directly dependent on modifications of the electrode properties. The values of the current densities obtained with the temporarily polarized electrode, which has been immersed in the anodic tank for 35 days, were smaller than the values measured on the continuously polarized clean electrode. The $t^{-0.5}$ evolution seems consistent with an evolution of the kinetic features of the electrode that may be due to the thickening of the passive layer (Evans, 1948).

In the literature, graphite anodes embedded in sediments have been reported to show sulphur deposits due to the electrochemical oxidation of sulphide (Eq. (1)), leading to S^0_{romb} rhombohedric crystal state ([Berner, 1963] and [Ryckelinck et al., 2005]). This deposit may mask a part of the active surface area and thus result in decreasing the electrode effectiveness. Nevertheless, sulphide deposits have generally been observed after longer operation times, 120 (Orfei et al., 2006) or 224 days (Tender et al., 2002), while here the anode lost its efficiency after only one day operation. The small stainless steel electrode (2.5 cm^2) that was put in the anode tank on day 35 was kept under constant polarization at −0.10 V vs. Ag/AgCl during four days, while a similar control coupon was kept in open potential. The surface composition of both electrodes was analyzed by EDS. The same quantity of sulphur was present in both samples. Sulphur precipitation was consequently not enhanced by four day polarization at −0.10 V vs. Ag/AgCl. This confirmed that sulphur deposit that may occur on the anode surface during cell operation cannot explain the decrease in efficiency.

Two other stainless steel electrodes, 15 cm^2 surface area each, were placed in the anode tank of the microbial fuel cell and continuously polarized for three weeks at, −0.45 V vs. Ag/AgCl and −0.15 V vs. Ag/AgCl, respectively. As shown in Fig. 3A, the value of −0.45 V vs. Ag/AgCl was close to the open circuit potential in this environment, while −0.15 V vs. Ag/AgCl corresponded to an operating potential value where the cell provided high current densities. The surface of stainless steel is known to be covered by a layer of oxides and hydroxides that gives the material its passive properties. The composition and features of the oxide layer depends on many different parameters such as the nature of the steel, composition of the medium, operating parameters, etc. Its conductive properties can vary to a great extent from full conductivity to p-type or n-type semi-conductor. The capacity of the passive layer C_{pl} of both stainless steel electrodes was measured by impedance spectroscopy as a function of the potential. The measurements at single frequency (1592 Hz) for each potential value took only a few seconds and were assumed not to disturb the passive layer. Variations of C_{pl}^{-2} are reported in Fig. 5 as a function of the potential, according to the Mott–Schottky relationship. Fig. 5 shows that the electrode polarized at −0.45 V gave a rather flat slope indicating that the oxide layer behaves like a conductor. When the sample was polarized at −0.15 V, the positive slope of the curve indicated that the oxide layer on stainless steel behaves like an n-type semiconductor.

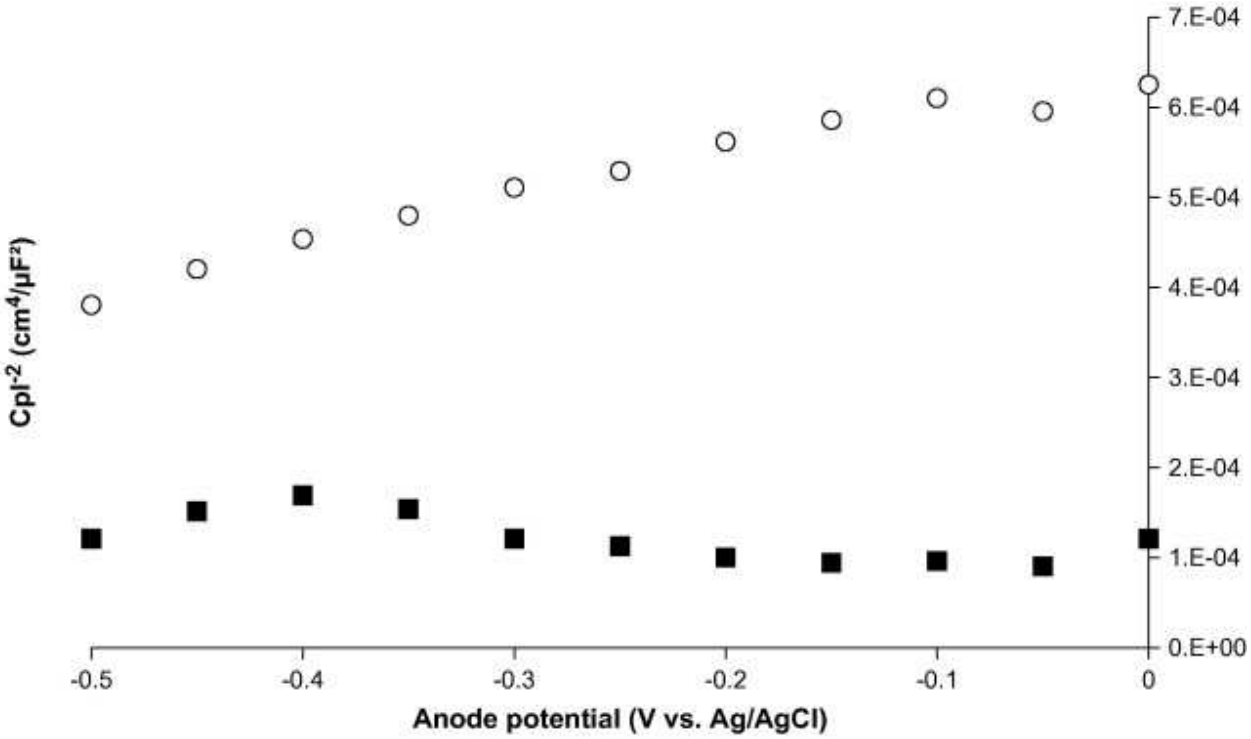

Fig. 5. Mott–Schottky plots of stainless steel polarized at −450 mV (■) and −150 mV vs. Ag/AgCl (○).

Formation of an n-type semi-conducting layer is very detrimental to the occurrence of an anodic process. Since the anode potential increased from around −0.45 V vs. Ag/AgCl at open circuit to around −0.15 V or more when the cell was in operation, it resulted in the modification of the oxide layer from a conductive behaviour towards n-type properties, which caused the power supply to decrease. When the cell was left at open circuit, the oxide layer partially recovered conductive properties, enabling the efficiency of the cell to be restored (Fig. 3A).

These results obtained in a complex natural environment were coherent with a previous study carried out in biochemical synthetic seawater (L'Hostis et al., 2003). The so-called "biochemical synthetic seawater" was chemical synthetic seawater supplemented with glucose and the enzyme glucose oxidase, which catalyzes the reduction of dissolved oxygen to hydrogen peroxide in the presence of glucose. The hydrogen peroxide produced, simulated in some extend the electrochemical effects of natural marine biofilms ([Dupont et al., 1998] and [Scotto et al., 1996]). In this medium, the open circuit potential of stainless steel AISI 316 L has been shown to increase from +0.20 to +0.35 V vs. SCE simultaneously to the evolution of the passive layer to n-type semi-conductive properties (L'Hostis et al., 2003).

The experiments conducted with constant and periodical polarizations and Mott–Schottky measurements suggested that oxide layer evolution was responsible for the behaviour of the anode. It should be concluded that stainless steel is not suitable in the anode process of marine fuel cells if the potential of the anode may be shifted to high values far from the open circuit potential.

As shown on Fig. 2, the biofilm-covered cathode here revealed less effective than obtained previously (Bergel et al., 2005). The presence of grazing protozoa in the seawater tank may drastically affect cathode biofilm. The maximum power that could be supplied by the MFC

prototype in optimal conditions may be assessed by coupling the graphite performances with the cathode features that were reported previously (Bergel et al., 2005). Coupling this cathode (25 mA at 0.08 V/AgAgCl) to the graphite anode from the study presented here (Fig. 2, 25 mA at −0.20 V/AgAgCl) would result in power supplied up to 0.35 W/m^2 with a 0.02 m^2-anode.

4. Conclusions

An experimental model, coming from the domain of anaerobic biocorrosion, was adapted here to design a lab MFC working in conditions close to sediment/seawater environments. The lab MFC can be implemented with only low quantity of sediment (0.2 l) and allows multiplying experimental attempts in well controlled conditions. The power density obtained cannot be straightforwardly compared to field results, mainly because of milk addition and the liquid condition in the anode tank (instead of compact sediments). Nevertheless, the anode behaviour in terms of open circuit potential was similar to what has been observed with benthic MFCs. Moreover, the microbial population present in the anode compartment revealed able to adapt to the milk consumption easily. The fact that seawater bacteria adapted easily to milk in a MFC, let think that sediments could be efficient inoculums to design MFC suitable for the treatment of dairy wastes. Indeed, the carbon concentration in dairy wastes is around three times higher than in domestic wastewater (Moletta and Torrijos, 1999). It may open a promising track to design efficient MFC that produces electricity from dairy wastes and simultaneously enhances their treatment. Work is now in progress in this direction with higher surface/volume ratios to increase the transformation ratios.
The model set-up allowed maintaining 0.10 W/m^2 during 45 days with a graphite anode, and it led to identify the cause of limitation of the stainless steel anodes. Actually, stainless steel showed correct kinetics features to support electrochemically active biofilms of *Geobacter sulfurreducens* in oxidation (Dumas et al., 2008). The detrimental evolution of the semi-conducting properties observed here may consequently be strongly dependent on the nature of the solution. This work should initiate further investigations on the evolution of the kinetics features of stainless steel with respect to the culture media, before to conclude definitively on the suitability or not of stainless steel as anode in MFC.

Acknowledgements

We are very grateful to Dr. Marco Faimali of CNR-ISMAR for his kind and efficient contributions and to Marc Roy of CEA-Saclay for the supply of stainless steel electrodes.

References

Angenent et al., 2004 L.T. Angenent, K. Karim, M.H. Al-Dahhan, B.A. Wrenn and R. Domiguez-Espinosa, Production of bioenergy and biochemicals from industrial and agricultural wastewater, *Trends Biotechnol.* **22** (2004), pp. 477–485.

Bergel et al., 2005 A. Bergel, D. Feron and A. Mollica, Catalysis of oxygen reduction in PEM fuel cell by seawater biofilm, *Electrochem. Commun.* **7** (2005), pp. 900–904.

Berner, 1963 R.A. Berner, Electrode studies of hydrogen sulphide in marine sediments, *Geochim. Cosmochim. Acta* **27** (1963), pp. 562–575.

Dupont et al., 1998 I. Dupont, D. Féron and G. Novel, Effect of glucose oxidase activity on corrosion potential of stainless steel in seawater, *Int. Biodeterior. Biodegrad.* **41** (1998), pp. 13–18.

Dumas et al., 2007 C. Dumas, A. Mollica, D. Féron, R. Basséguy, L. Etcheverry and A. Bergel, Marine microbial fuel cell: Use of stainless steel electrodes as anode and cathode materials, *Electrochim. Acta* **53** (2007), pp. 468–473.

Dumas et al., 2008 C. Dumas, R. Basséguy and A. Bergel, Electrochemical activity of *Geobacter sulfurreducens* biofilms on stainless steel anodes, *Electrochim. Acta* **53** (2008), pp. 5235–5241.

Evans, 1948 Evans, U.R., 1948. Metallic Corrosion – Passivity and Protection, London.

Jorgensen, 1977 B.B. Jorgensen, The sulphur cycle of a coastal marine sediment, *Limnol. Oceanogr.* **22** (1977), pp. 814–832.

L'Hostis et al., 2003 V. L'Hostis, C. Dagbert and D. Féron, Electrochemical behavior of metallic materials used in seawater-interactions between glucose oxidase and passive layers, *Electrochim. Acta* **48** (2003), pp. 1451–1458.

Liu and Logan, 2004 H. Liu and B.E. Logan, Electricity generation using an air–cathode single chamber microbial fuel cell in the presence and absence of a proton exchange membrane, *Environ. Sci. Technol.* **38** (2004), pp. 4040–4046.

Logan and Regan, 2006 B.E. Logan and J.M. Regan, Electricity-producing bacterial communities in microbial fuel cells, *Trends Microbiol.* **14** (2006), pp. 512–518.

Logan et al., 2006 B.E. Logan, B. Hamelers, R. Rozendal, U. Schroder, J. Keller, S. Freguia, P. Aelterman, W. Verstraete and K. Rabaey, Microbial fuel cells: methodology and technology, *Environ. Sci. Technol.* **40** (2006), pp. 5181–5192.

Lovley, 2006a D.R. Lovley, Bug juice: harvesting electricity with microorganisms, *Nat. Rev. Microbiol.* **4** (2006), pp. 499–508.

Lovley, 2006b D.R. Lovley, Microbial fuel cells: novel microbial physiologies and engineering approaches, *Curr. Opin. Biotechnol.* **17** (2006), pp. 1–6.

Lowy et al., 2006 D.A. Lowy, L.M. Tender, J.G. Zeikus, D.H. Park and D.R. Lovley, Harvesting energy from the marine sediment–water interface II: kinetic activity of anode materials, *Biosens. Bioelectron.* **21** (2006), pp. 2058–2063

Moletta and Torrijos, 1999 Moletta, R., Torrijos, M., 1999. Impact environnemental de la filière laitière. Techniques de l'ingénieur, traité Génie des Procédés, F1500.

Mollica, 2000 Mollica, M., 2000. Report of CREVCORR European Project, Cadarache.

Orfei et al., 2006 L.H. Orfei, S. Simison and J.P. Busalmen, Stainless steels can be cathodically protected using energy stored at the marine sediment/seawater interface, *Environ. Sci. Technol.* **40** (2006), pp. 6473–6478.

Park et al., 2005 H.I. Park, D.K. Kim, Y.-J. Choi and D. Pak, Nitrate reduction using an electrode as direct electron donor in a biofilm reactor, *Proc. Biochem.* **40** (2005), pp. 3383–3388

Rabaey et al., 2004 K. Rabaey, N. Boon, S.D. Siciliano, M. Verhaege and W. Verstraete, Biofuel cells select for microbial consortia that self-mediate electron transfer, *Appl. Environ. Microbiol.* **70** (2004), pp. 5373–5382.

Rabaey et al., 2003 K. Rabaey, G. Lissens, S.D. Siciliano and W. Verstraete, A microbial fuel cell capable of converting glucose to electricity at high rate and efficiency, *Biotechnol. Lett.* **25** (2003), pp. 1531–1535.

Rabaey and Verstraete, 2005 K. Rabaey and W. Verstraete, Microbial fuel cells: novel biotechnology for energy generation, *Trends Biotechnol.* **23** (2005), pp. 291–298.

Reimers et al., 2006 C.E. Reimers, P. Girguis, H.A. Stecher, L.M. Tender, N. Ryckelynck and P. Whaling, Microbial fuel cell energy from an ocean cold seep, *Geobiology* **4** (2006), pp. 123–136.

Reimers et al., 2001 C.E. Reimers, L.M. Tender, S. Fertig and W. Wang, Harvesting energy from the marine water interface, *Environ. Sci. Technol.* **35** (2001), pp. 192–195.

Rhoads et al., 2005 A. Rhoads, H. Beyenal and Z. Lewandowski, Microbial fuel cell using anaerobic respiration as an anodic reaction and biomineralized manganese as a cathodic reactant, *Environ. Sci. Technol.* **39** (2005), pp. 4666–4671.

Ryckelinck et al., 2005 N. Ryckelinck, H.A. Stecher and C.E. Reimers, Understanding the anodic mechanism of a seafloor fuel cell: interactions between geochemistry and microbial activity, *Biogeochemistry* **76** (2005), pp. 113–139.

Scotto et al., 1996 V. Scotto, A. Mollica, J.P. Audouard, C. Compère, D. Féron, D. Festy, T. Rogne, U. Steinsmo, C. Taxen and D. Thierry, Seawater Corrosion of Stainless Steels, The Institute of Materials (1996).

Tender et al., 2002 L.M. Tender, C.E. Reimers, H.A. Stecher, D.E. Holmes, D.R. Bond, D.A. Lowy, K. Piblobello, S. Fertig and D.R. Lovley, Harnessing microbially generated power on the seafloor, *Nat. Biotechnol.* **20** (2002), pp. 821–825.

Published in :

Bioresource Technology
Volume 99, Issue 18, December 2008, Pages 8887-8894